Proceedings of the 7th International Young Geotechnical Engineers Conference – Scott (Ed.)

Lateral spreading prediction for induced earthquakes

Prédiction de étalement latéral suite à des séismes induits

Jos de Greef & Floris Besseling
Witteveen+Bos Consulting Engineers, The Netherlands, jos.de.greef@witteveenbos.com

ABSTRACT: Lateral spreading is the phenomenon in which a sloping soil deposit displaces horizontally, due to a combination of earthquake-induced inertia forces and liquefaction. This type of displacement can be very destructive to the built environment as the horizontal deformation capacity of infrastructural objects and buildings is often limited. The currently available methods to predict the horizontal displacement are often of semi-empirical nature. Fitting parameters of such methods are derived from multivariate regression analyses using tectonic earthquake lateral spreading databases. Application of such methods to short duration, induced earthquakes such as occurring in Groningen, in general gives erroneous results. To answer whether lateral spreading is a phenomenon relevant to Groningen and what displacement magnitudes may be expected, in this study two available semi-empirical methods are combined. This allows for an indicative prediction of the horizontal displacement using subsoil-, geometry-, and seismic demand input parameters that are relatively easily accessible.

RÉSUMÉ : L'étalement latéral est le phénomène par lequel un dépôt de pente se déplace horizontalement, en raison des forces d'inertie et de liquéfaction générées suite à des séismes induits. Ce type de étalement latéral peut être très destructrice pour l'environnement bâti étant donné que la capacité de déformation horizontale des infrastructures et des bâtiments est souvent limitée. Les méthodes actuellement disponibles pour prédire l'étalement latéral sont souvent de nature semi-empirique. Les paramètres d'ajustement de ces méthodes sont dérivés d'analyses de régression multidimensionnelle utilisant des bases de données de étalement latérales suite à de séismes tectoniques. L'application de ces méthodes à des séismes induits de courte durée, comme celui de Groningen (Pays-Bas), donne généralement des résultats erronés. Pour savoir si l'étalement latéral est un phénomène pertinent pour Groningen et quelles magnitudes de déplacement horizontal peuvent y être attendues, deux méthodes semi-empiriques sont combinées dans cette étude. En utilisant les paramètres d'entrée du sous-sol, de la géométrie et de la sismique qui sont relativement facilement accessibles, cela permet une prédiction indicative du déplacement horizontal du sol.

KEYWORDS: lateral spreading, liquefaction, induced earthquakes

1 INTRODUCTION

Lateral spreading is the phenomenon in which a sloping soil deposit displaces horizontally, due to a combination of earthquake-induced inertia forces and liquefaction. This type of displacement can be very destructive to the built environment as the horizontal deformation capacity of infrastructural objects and buildings is often limited (see Figure 1).

The goal of our study is to identify, based on a literature study, whether lateral spreading can occur at canals and ditches in the province of Groningen, given the shallow (focal depth ~ 3 km), short duration earthquakes induced by gas extraction.

In general the methods available in literature to predict lateral spreading displacement magnitudes are semi-empirical relations that are substantiated by case history data from tectonic earthquakes. Applying these without further consideration leads to predicted displacement larger than deemed likely for induced short duration earthquakes in Groningen.

Several expressions for lateral spreading deformations by different researchers have been reviewed and combined to obtain an appropriate estimate for induced earthquakes. As a significant amount of Cone Penetration Test (CPT) data is readily available in the Groningen region, a precondition is that the geotechnical input for the estimate can be obtained from CPT.

2 DEFINITION

To be able to distinguish lateral spreading from other earthquake-related ground displacement phenomena, a definition is provided from Kramer (2013): *Lateral spreading is the finite, lateral movement of gently to steeply sloping, saturated soil deposits caused by earthquake-induced liquefaction*.

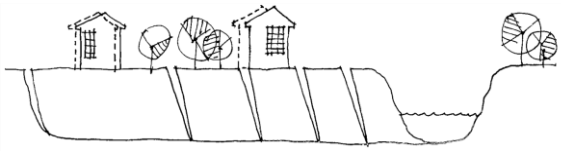

Figure 1. Schematic visualization of lateral spreading (BRANZ, 2021)

Rather than using the term slope, levee or river bank, in literature the term free face is adopted. Bartlett and Youd (1995) explain the term as an abrupt topographical depression but no actual definition of the steepness is provided in literature. As presented later on, in the prediction models lateral spreading displacements are a function of distance from the free face toe, rather than its steepness.

By using above definition of lateral spreading, it distinguishes from (a) finite inertial instability displacements without shear strength reduction which can be quantified by performing Newmark or non-linear dynamic finite element analyses and (b) flow failure displacements of which it is difficult to accurately quantify the displacements. Identifying the latter mechanism is possible by assessing the stability near free faces using post-liquefaction residual strengths, e.g. Idriss and Boulanger (2008), Kramer and Wang (2015). From a more fundamental perspective Youd (1973) describes above phenomena by referring to the behavior observed in static- and cyclic laboratory tests.

Due to topographic- and soil heterogeneity in practice often a combination of lateral spreading and flow failure (or slumping) mechanisms is observed. Cubrinovski et al. (2012) make a distinction between a ‘block-mode’ failure and an ‘exponential-decay’ ground deformation pattern near Kaiapoi, New Zealand, following the 2010 Darfield earthquake. The former shows the horizontal movement of a near intact soil body, the latter shows large horizontal deformations near the waterway which

exponentially decreases at increasing distance from the river bank. Close to the river bank it is likely that multiple mechanisms play a role simultaneously. Zhang et al. (2004) note the mechanisms of lateral spreading and local slumping failure are fundamentally different. That is why they have removed from their lateral spreading case history database all instances in which the distance from the (toe of the) free face is smaller than four times the free face height.

3 PREDICTION METHODS

As the consequences of lateral spreading can be so devastating, numerous studies on the subject have been performed varying from centrifuge tests to advanced numerical modelling. In this section several available prediction methods are presented their (dis-)advantages are discussed. This mainly with respect to application to induced earthquakes in Groningen.

3.1 *Hamada (1999)*

Hamada et al. (1987) propose an empirical relation to estimate the liquefaction induced horizontal ground displacement D_H as a function of the thickness of the liquefied soil layer H_{liq} [m] and the slope of the surface S [%]. This relation is based on ground displacement vectors during the 1964 Niigata and 1983 Nihonkai-Chubu earthquakes in Japan.

Hamada (1999) extends this relation to Equation (1) below. Herein the acceleration time history is included using A_i [gal] representing the maximum acceleration in the n^{th} segment of the acceleration time history and T_i [s] the duration of the n^{th} segment. The soil condition of the liquefied layer is represented by the normalized SPT value N [-] which is approximately equal to $(N_1)_{60}$ [-].

$$D_H = \frac{0.0125 \cdot \sqrt{H_{liq}} \cdot S}{\bar{N}^{0.88}} \cdot \sum_i^n A_i^{0.48} T_i \qquad (1)$$

Using Equation (1) a measured or fitted acceleration time history can be used to predict lateral displacements. In absence of reliable or easy-defined attenuation relationships this is a pro, in many cases this will be a con as no acceleration time histories are available. The definition of H_{liq} assumes there is one liquefiable layer. It is not quite clear how to interpret this value in the case of layered soil deposits in which some layers are not susceptible to liquefaction.

3.2 *Youd et al. (2002)*

Bartlett & Youd (1992, 1995) performed a statistical analysis on observed lateral spreading sites observed after 8 major earthquakes in Japan and the United States reported in several NCEER reports, e.g. Hamada and O'Rourke (1992). Using a multi-linear regression analysis two empirical models are set up that can be used to predict the displacement; one for gently sloping ground conditions and one for free face conditions. Youd et al. (2002) revised this empirical model by implementing some updates on the functional form of the prediction equation, the reassessment of same data and the addition of data from three other earthquakes. The resulting prediction equations are often referred to and contain terms for the earthquake intensity, geotechnical characteristics and local geometry. Importantly, only the local geometry term and a fitting constant vary when considering either gently sloping ground or free face conditions.

Important assumption in deriving above two relations by Youd et al. (2002) is the implicit attenuation relation that limits applicability to stiff sites in Japan and the western part of the United States. For soft soil sites at which significant amplification is expected, an equivalent distance term R_{eq} can be obtained from Figure 2 which represents an average from three different attenuation relations. This attenuation however still applies to tectonic earthquakes, whereas the induced earthquakes in Groningen have a limited focal depth of ~ 3km. As Bommer and Van Elk (2017) note that the modal expected maximum magnitude M_{max} in Groningen is 4.5, it is moreover evident that extrapolation of the curves in Figure 2 would be required.

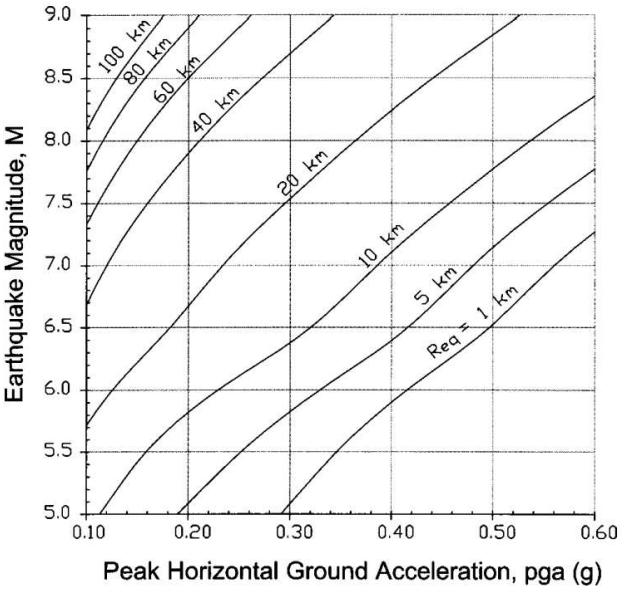

Figure 2. Graph presented by Youd et al. (2002) to obtain the equivalent source distance R_{eq} in case of soft soil sites

Franke & Stewart (2014) incorporate the method by Youd et al. (2002) in a probabilistic framework to be able to combine all possible earthquake scenarios and their weighted likelihood. Hereby the robustness to the large sensitivity to M and R is increased, albeit at the cost of computational effort. They moreover note that the standard deviation on a log-scale from the Youd et al. (2002) procedure is 0.197 on log scale which in terms of predicted settlement implies coefficient of variation of 0.57.

Zhang & Zhao (2005) note that the database of magnitudes and source distances underlying the method by Youd et al. (2002) is poorly distributed and that different faulting mechanisms may have an effect. They moreover note that the database is dominated by the Niigata 1964 earthquake as most displacement vectors where measured at that event (see Figure 3).

Figure 3. Permanent ground displacement vectors in the upstream area of the Shinano River after the 1964 Niigate earthquake (from: Hamada and O'Rourke (1992))

3.3 *Rauch (1997)*

Rauch (1997) comprised a large database of in total 78 independent lateral spreading events (or slide areas), observed during 16 earthquakes over the period 1906 - 1994. Per location as much as 70 types of descriptive types of information were defined, e.g.: earthquake name, location, magnitude, peak ground acceleration, thickness of the liquefied layer, ground slope, observed displacement magnitude, etc. The various displacement vectors and site investigation points at one event are combined, giving a mean and standard deviation for these parameters.

Using a multi-linear regression analysis the compiled data was used to set up a model to predict the magnitude of the horizontal displacement. Since not all descriptive information was available at all sites, a rough-to-fine model set-up was used: at first a regional component is defined if only seismic loading parameters are known. Secondly a site component containing geometrical aspects can be added and thirdly a geotechnical component containing geotechnical information can be added.

The method proposed by Rauch (1997) yields larger displacements with increasing M and smaller displacements with increasing R. This makes sense: the stronger the earthquake and the closer one is to the source, the larger the expected displacements. However, through the multi-variate regression analysis smaller displacements are predicted with increasing maximum acceleration and duration. Although acknowledged, it is stated by Rauch (1997) that this does not have an adverse effect on model outcome. It does however imply that the model can only be used to obtain an approximate value of the displacement, it is not possible to perform a sensitivity analyses. This may in particular be a problem for small expected displacements as for the regional model the minimum displacement is 14.9 cm.

To include the site component, the expected length of the sliding plane is required, which is a difficult parameter to know a-priori. One can imagine that the closer to the free face, the larger the expected displacement. This behavior is however not obtained by adopting the method by Rauch (1997) as a larger displacement is predicted if the lateral spread length is larger too.

3.4 *Zhang et al. (2004)*

Zhang et al. (2004) propose to link the observed horizontal lateral displacement to a combination of a one-dimensional liquefaction severity index and simply geometric parameters. The severity index used is the Lateral Displacement Index (LDI) which is a depth-integrated measure of the (liquefied) strain potential of the soil column. The geometric parameter is either the slope S [%] in absence of a free face and the ratio L/H for free face conditions where H [m] is the free face height and L [m] the distance behind the toe of the slope. For verification of this procedure 13 case histories during 12 earthquakes are used, see e.g. Figure 4.

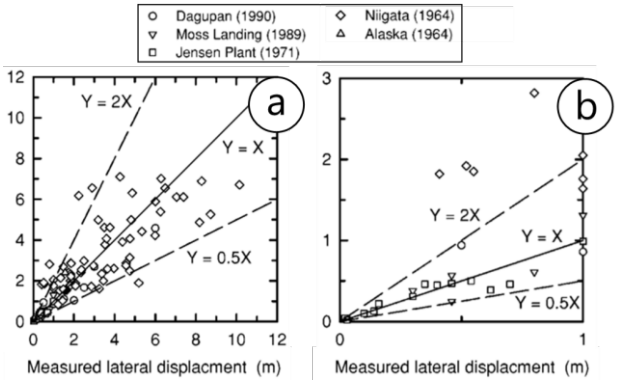

Figure 4. Comparison of measured and calculated lateral displacements by Zhang et al. (2004) for free facing ground conditions (a) full data set (b) data with measured displacements up to 1 meter

A selection procedure was used to exclude cases that were not 'purely' lateral spreading because of e.g. impeded displacements by boundary effects, multiple possible failure mechanisms, high static shear stresses that may have caused local slump and/or flow failure.

Like Youd et al. (2002) the individual displacement vectors were used to assess the proposed model performance. The model performance is shown in Figure 4 where it is noted that the two free face datasets on the right are eventually combined which appears to be justified for slopes up to 0.5%.

3.5 *Valsamis et al. (2010)*

Valsamis et al. (2010) performed a variety of dynamic numerical analyses in FLAC using a material model that allows for the generation of excess pore pressures and thus the onset of liquefaction. The numerical model is calibrated by back-calculating centrifuge tests after which parameter variation studies are performed. The results from the latter are then regressed to obtain empirical relations that can be used to estimate horizontal displacements, see Equation 2. Herein a_{mean} [g] is the mean acceleration, $T(N_{cyc}\text{-}N_L)$ [s] the duration of strong shaking after the onset of liquefaction, $(N_1)_{60cs}$ [-] the (clean sand corrected) normalized SPT value, H_{tot} [m] the depth to the sliding plane, i [°] the ground surface inclination and FC the fines content of the liquefied layer.

$$D_H = 2.1 \cdot \left(\frac{a_{mean}}{g}\right)^{0.5} \cdot \left[T\left(N_{cyc} - N_L\right)\right]^{0.8} \cdot \left[(N_1)_{60cs}\right]^{-1} \cdot [H_{tot}] \cdot \left[\tan i\right]^{0.5} \cdot (1 - FC)^3 \quad (2)$$

The performance of Equation 2 is compared with the relation proposed by Hamada (1999) for several case histories, centrifuge experiments and the numerical simulations. For the case histories several assumptions were made for any missing parameters. In Figure 5 it can be observed that this in general appears to yield a less conservative result. The prediction variability on first sight (using calculated versus measured diagrams such as Figure 4) appears to be similar to the model by Youd et al. (2002), Rauch (1997) and Zhang et al. (2004).

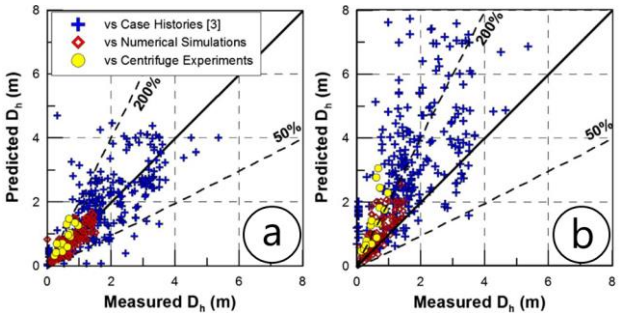

Figure 5. Accuracy of predicted ground surface displacement from case histories, centrifuge tests and numerical simulations: (a) for Equation 2 by Valsamis et al. (2010) (b) for Equation 1 by Hamada (1999).

4 APPLICATION TO INDUCED EARTHQUAKES

All mentioned prediction methods have their limitations which introduces a non-quantified uncertainty when applying them to Groningen conditions. In this paragraph different favourable aspects of the methods are combined to overcome the most important limitations.

4.1 *Use of acceleration time history*

The attenuation relationships that are (implicitly) used in the prediction methods introduce an unquantified uncertainty when applied to induced earthquakes with a small focal depth (~ 3 km).

For this reason plus the fact that (design) acceleration time histories are available in Groningen, there is a preference to use a prediction method in which the acceleration time history can be used as input. This leaves the methods by Hamada (1999) and Valsamis et al. (2010) as viable options. These methods were derived for gently sloping surface inclinations S [%].

As SPT values are not commonly used in The Netherlands, the term $N^{0.88}$ from Equation 1 is converted to a term containing the relative density. For this purpose the relation between normalized SPT blowcount and relative density by Idriss and Boulanger (2008) is used. The resulting term is $D_R^{1.76}/114$ with D_R in %. This leads to Equation 3.

$$D_{H;Ham}(S) \approx \frac{\sqrt{H_{liq}}\cdot S}{0.7 D_R^{1.76}} \cdot \sum_i^n A_i^{0.48}\, T_i \qquad (3)$$

In Equation 2 the surface inclination is represented by i (=S/100). In general for the considered slopes i << 1, therefore [tan i] ≈ i and $[\tan i]^{0.5} \approx S^{0.5}/10$. As the exact moment liquefaction occurs is unknown, the duration of strong shaking after the onset of liquefaction, $T(N_{cyc}\text{-}N_L)$, is replaced by the duration of strong shaking D [s]. This duration is defined as the period between the last and first exceedance of 0.05g in accordance with Rauch (1997). Using the same relation between SPT blowcount and relative density this leads to Equation 4.

$$D_{H;Val}(S) \approx \frac{\sqrt{a_{mean}}\cdot D^{0.8}\cdot H_{tot}\cdot\sqrt{S}\cdot(1-FC)^3}{0.0219\cdot D_R^2} \qquad (4)$$

4.2 *Equivalence of infinite slopes and free face*

The methods by Hamada (1999) and Valsamis et al. (2010) are derived for gently sloping ground conditions, whereas it was mentioned the goal of this study was to evaluate performance of ditches and canals, thus free face conditions.

Since Youd et al. (2002) and Zhang et al. (2004) propose prediction methods that can be applied to both conditions, it is possible to derive curves that represent equal displacements, provided that only the geometry of the problem is different.

These equivalent curves are presented in Figure 6 and Figure 7. The solid part of the curves show the validity range of the curves. For the method by Youd et al. (2002) these are slopes for which 0.1% ≤ S ≤ 6.0% and free facing conditions for which 1% ≤ H/L ≤ 20%. For the method by Zhang et al. (2004) these are slopes for which 0.2% ≤ S ≤ 3.5% and free facing conditions for which 4 ≤ L/H ≤ 40.

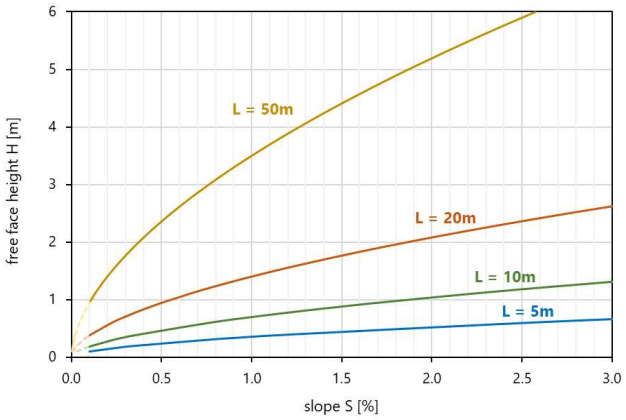

Figure 6. Equivalence between slope S [%] and free face height H [m] at different distances behind the toe of the slope L [m] using the prediction equations by Youd et al. (2002)

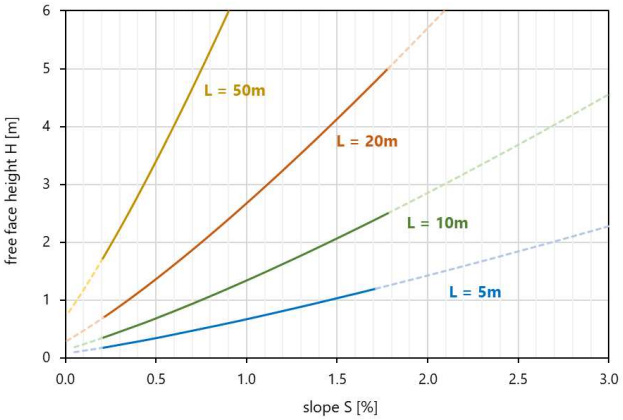

Figure 7. Equivalence between slope S [%] and free face height H [m] at different distances behind the toe of the slope L [m] using the prediction equations by Zhang et al. (2004)

4.3 *Issues related to liquefaction*

One of the preconditions of lateral spreading, by definition, is the occurrence of liquefaction. Whether (significant) liquefaction is at all possible in Groningen at design earthquake conditions, is still a subject that is open for debate. To date no seismic liquefaction has been observed in the region. Green (2018) set up a Groningen-specific liquefaction triggering procedure that accounts for the typical soil profiles encountered in the region and the short duration nature of the earthquakes, respectively by introducing a custom shear stress reduction factor r_d and Magnitude Scaling Factor (MSF) in addition to the existing CPT based liquefaction procedure by Boulanger and Idriss (2015).

Youd (2018) mentions that for liquefied layers less than 30 cm, CPT based methods generally result in an overprediction of lateral displacement as in deltaic regions such layers are seldomly continuous. One of the aspects missing from the databases is the inclusion a very small magnitude lateral spread displacements. In general, the case history database contains mainly cases in which large displacements were found, after which site investigations were performed. There are very few cases in which no displacement was observed, where in reality large displacements were to be expected. One of these cases is found in Turkey during the 1999 Kocaeli earthquake and it touches on the same issue often encountered in Groningen: the liquefaction susceptibility of layered and interbedded soils. Although Boulanger et al. (2016) conclude that a correction for transition- and thin layer effects is not sufficient to mitigate the overprediction, it does help to reduce bias.

De Greef and Lengkeek (2018) proposed a spreadsheet-based thin-layer correction procedure, based on the commonly cited equation by Youd et al. (2001). Based on recent laboratory test results on penetration resistance in multiple layered soils by De Lange (2018) an addition to this relation is proposed to account for larger corrections 1.8 at low H/d_{cone} ratios, see Figure 8.

It is proposed to use Equation 5 if $H/d_{cone} > 4$ and to use Equation 6 if $H/d_{cone} \leq 4$. Herein z represents the shortest vertical distance to a cohesive layer either on top- or below the interbedded layer of interest. Equation 6 is empirically fitted to the curves in Figure 8 at exceedance probabilities P of 15%, 50% and 85%.

$$K_Z = 1 + 0.25\left(\frac{1}{17}\left(\frac{2z}{d_c}\right) - 1.77\right)^2 \qquad (5)$$

$$K_Z = 1.54 + 6.0\exp\left\{0.39\cdot\Phi^{-1}(P) - 1.2\left(\frac{2z}{d_c}\right)\right\} \qquad (6)$$

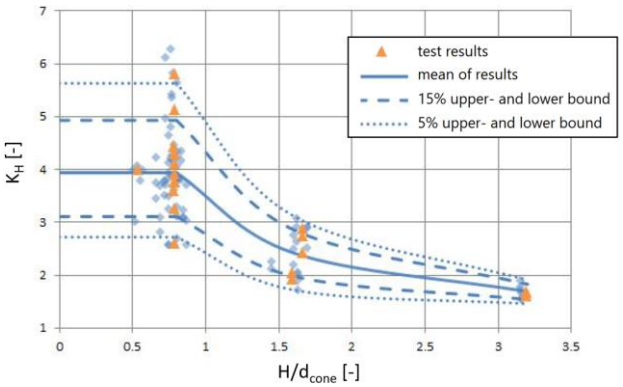

Figure 8. Derived correction factors K_H as function of the H/d_{cone} ratio as derived from test results by De Lange (2018)

5 CASE STUDY ANALYSIS

For a quantitative analysis a case study analysis was performed, using conservative (but not necessarily worst-case) conditions, as to guarantee non-zero displacements.

In total 11 two-component design acceleration time histories were selected, with a scaled peak ground acceleration (PGA) equal to 0.20g (return period 2,475 years). The average strong-motion duration was 4.2 seconds (CoV = 0.36). The mean acceleration during this duration was 0.043g (CoV = 0.10).

A highly liquefaction susceptible soil profile was selected, see Figure 9, with a high water table of 50 cm below surface level. First a transition- and thin layer correction was performed using Equation 5 and Equation 6. Secondly, the liquefaction triggering procedure proposed by Green (2018) was performed, resulting in the cyclic resistance ratios (CRR) and liquefaction safety factors (FS_{liq}) presented in Figure 10.

To obtain the liquefied layer thickness H_{liq} the cumulative thickness of soil layers that liquefy is used. The depth to the sliding plane H_{tot} was estimated at 6 m as this is the deepest occurrence at which the soil is expected to liquefy. The average fines content of the liquefied layer is estimated by using the relation between soil behavior type index I_c and FC proposed by Boulanger and Idriss (2015), using $C_{FC} = 0$.

A fictive slope with a height H of 3m and a steepness of 1:3 was assumed, which are typical dimensions for ditches and small canals in Groningen.

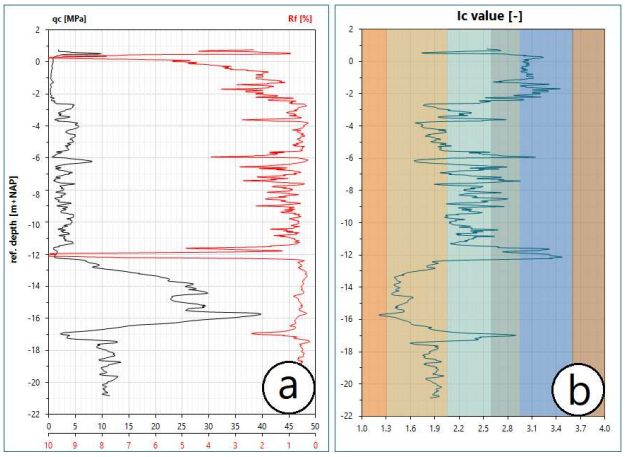

Figure 9. Case study soil profile: (a) measured cone resistances and friction ratios (b) SBTn soil behaviour type index

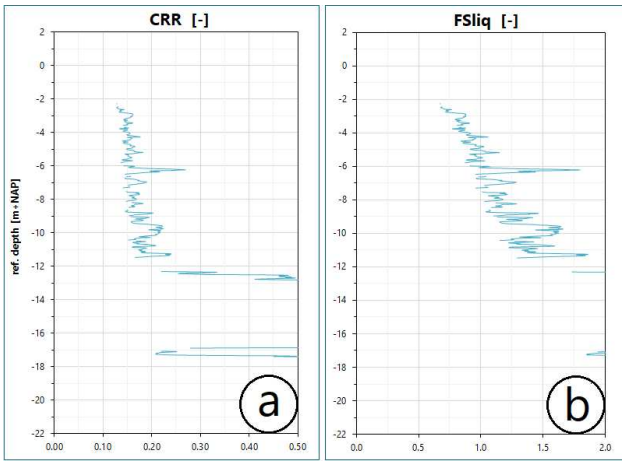

Figure 10. Case study liquefaction analysis: (a) cyclic resistance ratio (CRR) profile (b) liquefaction safety factor (FSliq) profile

An overview of the case study input parameters relevant as input to Equation 3 and Equation 4 are listed in Table 1.

Table 1. Summary of case history parameters

Parameter	*Symbol [unit]*	*Value*
Relative density liquefied layer	D_R [%]	52
Liquefied layer thickness	H_{liq} [m]	2.7
(Weighted) acceleration time history	$\Sigma A_i^{0.48} T_i$ [-]	40.6
Strong motion duration	D [s]	4.2
Mean acceleration in D	a_{mean} [g]	0.043
Depth to sliding plane	H_{tot} [m]	6
Fines content liquefied layer	FC [%]	19

Calculation results for these specific conditions are shown in Figure 11. Herein the parameter values from Table 1 are used as input in Equations 3 and 4 where the equivalent relations from Figures 6 and 7 are used to replace the slope steepness S by a combination of free face height H and toe distance L.

On the left vertical axis the predicted horizontal displacement magnitude D_H [cm] of different solid curves is shown. The right vertical axis represents the profile height H [m] depicted by the dashed curve. The shaded area on the left indicates the range in which L/H < 4 where mechanisms other than lateral spreading may be dominant according Zhang et al. (2004).

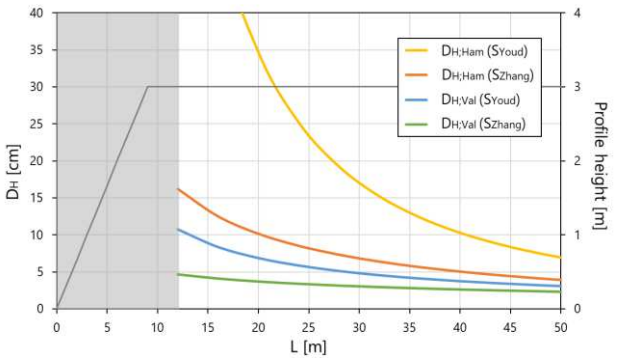

Figure 11. Calculated horizontal displacements D_H [cm] as a function of distance from the toe L [m] for case study input parameters

It can be observed that at L = 20 m the predicted horizontal displacement varies from 4 to 35 cm among the combined

methods. Although dependent on the different input parameters, the predicted displacements by Valsamis et al. (2010) are generally lower than by Hamada (1999). At very low fines content, which is not an explicit parameter in the latter method, $D_{H;Val}(S_{Youd}) > D_{H;Ham}(S_{Zhang})$.

Significantly the largest displacements are predicted by $D_{H;Ham}(S_{Youd})$ in particular at relatively short distances L. This observed exponential increase of the displacement is caused by a combination of factors. S_{Youd} inflates (far beyond the validity range of 6%) for high H/L ratios, which is shown by the near-horizontal curves in Figure 6. As the predicted horizontal displacement from Equation 3 depends linearly on S, the predicted displacements are thereby inflated as well.

6 DISCUSSION

To determine the expected horizontal displacement at free facing conditions in Groningen, an assessment is made using two methods that rely on the acceleration time history rather than earthquake magnitude M and epicentral distance R. Since these methods are derived for gently sloping ground conditions with a slope S, the slope is expressed as a function of free face height H and distance L using two different equal-displacement relations.

In this way four relations are obtained which can be used to indicatively quantify lateral displacements using subsoil-, geometry- and seismic demand input parameters that are relatively easily accessible in Groningen. For the presented case study there is a large variety in outcome between the four relations. The calculated displacements at design conditions are relatively low compared to the general absolute prediction accuracy of the underlying methods.

In the case study the seismic demand parameters at design earthquake conditions are on the lower end of the databases from literature: in nearly all instances the strong-motion durations in the databases are higher at similar to higher PGA levels. An exception is found in the database compiled by Rauch (1997) in which lateral displacements in excess of 1 m have been observed during the 1948 Fukui earthquake (D = 4 s, PGA = 0.25g) at sloping ground conditions.

Although no specific boundary conditions (subsoil, geometry, and seismic demand) have been identified that prohibit lateral spreading in Groningen, the occurrence probability is expected to be very low as the return period of the used design seismic load in the case study is 2,475 years and specifically a CPT was selected with a high liquefaction potential. As gas production in Groningen is scaled-down in recent and coming years, future seismic loads are accordingly expected to decrease.

For practical purposes it should be verified whether a liquefiable layer is horizontally continuous by performing multiple boreholes or CPTs. Moreover the location of the liquefiable layer compared to the slope should be considered, Youd (2018) provides some practical insights in this respect.

7 REFERENCES

Bartlett, S.F. and Youd, T.L. 1992. *Empirical Analysis of Horizontal Ground Displacement Generated by Liquefaction-Induced Lateral Spreads - Technical Report NCEER-92-0021*.

Bartlett, S.F. and Youd, T.L. 1995. Empirical Prediction of Liquefaction-Induced Lateral Spread. *Journal of Geotechnical Engineering*, 121(4): 316-329.

Bommer, J.J. and Van Elk, J. 2017. Comment on "The Maximum Possible and the Maximum Expected Earthquake Magnitude for Production-Induced Earthquakes at the Gas Field in Groningen, The Netherlands" by Gert Zöller and Matthias Holschneider, *Bulletin of the Seismological Society of America*, 107(3): 1564-1567.

Boulanger, R.W. and Idriss, I.M. 2015. CPT-Based Liquefaction Triggering Procedure. *Journal of Geotechnical and Geoenvironmental Engineering*, 142(2).

Boulanger, R.W., Moug, D.M., Munter, S.K., Price, A.B. and DeJong, J.T. 2016. Evaluating liquefaction and lateral spreading in the interbedded sand, silt and clay deposits using the cone penetrometer. *Australian Geomechanics*, 51(4): 109-128.

BRANZ Seismic resilience. http://www.seismicresilience.org.nz/topics/seismic-science-and-site-influences/earthquake-hazards/lateral-ground-displacement/, accessed 29 July 2021.

Cubrinovski, M., Robinson, K., Taylor, M., Hughes, M. and Orense, R. 2012. Lateral spreading and its impacts in urban areas in the 2010-2011 Christchurch earthquakes. *New Zealand Journal of Geology and Geophysics*, 55(3): 255-269.

De Greef, J. and Lengkeek, H.J. 2018. Transition- and thin layer corrections for CPT based liquefaction analysis. *Cone Penetration Testing 2018 - Papers*: 317-322.

De Lange, D. 2018. *CPT in Thinly Layered Soils - Validation Tests and Analysis for Multi Thin layer Correction*. Research Report for NAM.

Franke, K.W. and Kramer, S.L. 2014. Procedure for the Empirical Evaluation of Lateral Spread Displacement Hazard Curves. *Journal of Geotechnical and Geoenvironmental Engineering*, 140(1): 110-120.

Green, R.A. 2018. *Groningen-Specific Liquefaction Evaluation - Summary*. Background document to the 2018 version of the NPR9998.

Hamada, M. 1999. Similitude law for liquefied-ground flow. *Proceedings of the Seventh US-Japan Workshop on Earthquake Resistant Design of Lifeline Facilities and Countermeasures Against Soil Liquefaction*. Technical Report MCEER-99-0019: 191-205.

Hamada, M. and O'Rourke, T.D. 1992. *Case Studies of Liquefaction and Lifeline Performance During Past Earthquakes - Volume 1 Japanese case Studies*. Technical Report NCEER-92-0001.

Hamada, M., Towhata, I, Yasuda, S. and Isoyama, R. 1987. Study on permanent ground displacement induced by seismic liquefaction. *Computers and Geotechnics* 4: 197-220.

Idriss, I.M. and Boulanger, R.W. 2008. *Soil Liquefaction During Earthquakes*. EERI Monograph MNO-1.

Kramer, S.L. 2013. *Lateral Spreading.* In: Bobrowsky P.T. (eds) Encyclopedia of Natural Hazards. Encyclopedia of Earth Sciences Series. Springer, Dordrecht.

Kramer, S.L. and Wang, C. 2015. Empirical Model for Estimation of the Residual Strength of Liquefied Soil. *Journal of Geotechnical and Geoenvironmental Engineering*, 141(9).

Rauch, A.F. 1997. *EPOLLS: An Empirical Method for Predicting Surface Displacements Due to Liquefaction-Induced Lateral Spreading in Earthquakes* (PhD thesis), Blacksburg, Virginia, USA.

Valsamis, A.I., Bouckovalas, G.D. and Papadimitriou, A.G. 2010. Parametric investigation of lateral spreading of gently sloping liquefied ground. *Soil Dynamics and Earthquake Engineering* 30: 490-508.

Youd, T.L. 1973. Liquefaction, Flow and Associated Ground Failure. *Geological Survey Circular* 688.

Youd, T.L. 2018. Application of MLR Procedure for Prediction of Liquefaction-Induced Lateral spread displacement. *Journal of Geotechnical and Geoenvironmental Engineering*, 144(6).

Youd, T.L. Idriss, I.M, Andrus, R.D., Arango, I., Castro, G., Christian, J.T., Dobry, R., Finn, W.D.L, Harder Jr, L.F., Hynes, M.E., Ishihara, K., Koester, J.P., Liao, S.S.C., Marcuson III, W.F., Martin, G.R., Mitchell, J.K., Moriwaki, Y., Power, M.S., Robertson, P.K., Seed, R.B. and Stokoe II, K.H. 2001. Liquefaction Resistance of Soils: Summary Report from the 1996 NCEER and 1998 NCEER/NSF Workshops on Evaluation of Liquefaction Resistance of Soils. *Journal of Geotechnical and Geoenvironmental Engineering* 127(10): 817-833.

Youd, T.L., Hansen, C.M., Bartlett, S.F. 2002. Revised Multilinear Regression Equations for Prediction of Lateral Spread Displacement. *Journal of Geotechnical and Geoenvironmental Engineering*, 128(12): 1007-1017.

Zhang, G., Robertson, P.K. and Brachman, R.W.I. 2004. Estimating Liquefaction-Induced Lateral Displacements Using the Standard Penetration Test of Cone Penetration Test. *Journal of Geotechnical and Geoenvironmental Engineering*, 130(8): 861-871.

Zhang, J. and Zhao, J.X. 2005. Empirical models for estimating liquefaction-induced lateral spread displacement. *Soil Dynamics and Earthquake Engineering* 25: 439-450.